Linear Tricobalt Compounds with Di(2-pyridyl)amide (dpa) Ligands: Temperature Dependence of the Structural and Magnetic Properties of Symmetrical and Unsymmetrical Forms of $Co_3(dpa)_4Cl_2$ in the Solid State

Rodolphe Clérac,[†] F. Albert Cotton,*[,†] Lee M. Daniels,[†] Kim R. Dunbar,*[,†] Kristin Kirschbaum,[‡] Carlos A. Murillo,*[,†,§] A. Alan Pinkerton,[‡] Arthur J. Schultz,[||] and Xiaoping Wang[†]

Contribution from the Laboratory for Molecular Structure and Bonding, Department of Chemistry, Texas A&M University, P.O. Box 30012, College Station, Texas 77842-3012, Department of Chemistry, University of Toledo, Toledo, Ohio 43606, Department of Chemistry, University of Costa Rica, Ciudad Universitaria, Costa Rica, and the Intense Pulsed Neutron Source, Argonne National Laboratory, Argonne, Illinois 60439

Received February 11, 2000

Abstract: The linear trinuclear compound $Co_3(dpa)_4Cl_2$ (**1**; dpa = di(2-pyridyl)amide anion) crystallizes from CH_2Cl_2 solution in two forms simultaneously, namely, an orthorhombic form **1**·CH_2Cl_2 and a tetragonal form **1**·$2CH_2Cl_2$. The three linearly arranged cobalt atoms in **1** are supported by four dpa ligands in a spiral configuration. The chain of cobalt atoms is symmetrical in **1**·CH_2Cl_2, but unsymmetrical in **1**·$2CH_2Cl_2$. Both crystal structures have been studied at various temperatures. A reversible second-order phase transition (165 K) from orthorhombic (*Pnn*2) to monoclinic (*Pn*) symmetry for the crystal of **1**·CH_2Cl_2 has been documented by X-ray studies at 296, 168, and 109 K as well as a neutron diffraction study at 20 K. The linear tricobalt unit in **1**·CH_2Cl_2 becomes slightly unsymmetrical at low temperature although the two Co−Co bonds remain statistically equivalent (Co−Co ≈ 2.32 Å) throughout the experimental temperature range. No phase transition was observed for the tetragonal form **1**·$2CH_2Cl_2$ at low temperature, but the Co−Co distances in **1** changed from 2.299(1) and 2.471(1) Å at 298 K to 2.3035(7) and 2.3847(8) Å at 20 K. Magnetic susceptibility measurements indicate that the two compounds are in an $S = {}^1/_2$ ground state at low temperature and exhibit gradual spin-crossover at higher temperature.

Introduction

The compound $Co_3(dpa)_4Cl_2$ (**1**), where dpa represents the anion of di(2-pyridyl)amine, was first prepared by Peng and co-workers in 1994.[1] They proposed an unsymmetrical molecule, abbreviated as *u*-**1** (Chart 1), with Co−Co distances of 2.290(3) and 2.472(3) Å. The structure was explained by postulating one singly bonded dicobalt unit,[2] joined to an isolated square pyramidal Co^{II}-containing species. They also presented magnetic measurements that showed a magnetic moment which was constant at ∼1.8 μ_B from 5 to 150 K but then increased to ∼2.6 μ_B at 300 K. This was attributed to a temperature-dependent spin crossover behavior of the isolated Co^{II} atom, which would be going from an $S = {}^1/_2$ state toward an $S = {}^3/_2$ state as the temperature increased.

Chart 1

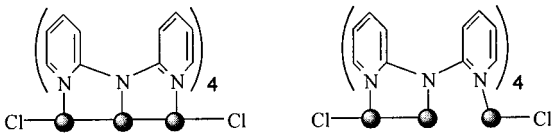

***s*-$Co_3(dpa)_4Cl_2$** ***u*-$Co_3(dpa)_4Cl_2$**

The situation seemed to be a closed story until work in this laboratory[3] in 1997 revealed that a molecule of exactly the same composition exists in a different crystalline form, namely *s*-**1**·CH_2Cl_2. In this structure, the molecule is completely symmetric, with equal Co−Co distances (2.3178(9) Å), and equal Co−Cl distances.

Further work[4] soon made it evident that the behavior of this molecule, or its derivatives, was even more unusual. First, it

* To whom correspondence should be addressed.
[†] Texas A&M University.
[‡] University of Toledo.
[§] University of Costa Rica.
[||] Argonne National Laboratory.

(1) Yang, E.; Cheng, M.; Tsai, M.; Peng, S. M. A. *J. Chem.* Soc., *Chem. Commun.* **1994**, 2377. A compound said to be **1**·$2CH_2Cl_2$·H_2O was reported in this paper to crystallize in space group *I*4. However, this should be *I*$\bar{4}$, based on the atomic coordinates retrieved from the Cambridge Crystallographic Data Centre. Since no details of this structure have ever been reported; the evidence, if any, for the presence of H_2O is obscure.

(2) (a) Cotton, F. A.; Poli, R. *Inorg. Chem.* **1987**, *26*, 3652. (b) He, L.-P.; Yao, C.-L.; Naris, M.; Lee, J. C.; Korp, J. D.; Bear, J. L. *Inorg. Chem.* **1992**, *31*, 620. (c) Cotton, F. A.; Daniels, L. M.; Feng, X.; Maloney, D. J.; Matonic, J. H.; Murillo, C. A. *Inorg. Chim. Acta,* **1997**, *256*, 291.

(3) Cotton, F. A.; Daniels, L. M.; Jordan, G. T., IV *Chem. Commun.* **1997**, 421.

(4) Cotton, F. A.; Daniels, L. M.; Jordan, G. T., IV.; Murillo, C. A. *J. Am. Chem. Soc.* **1997**, *119*, 10377. In two places in this paper the formula was given incorrectly as $Co_3(dpa)_4Cl_2$·$2CH_2Cl_2$. The correct formula is $Co_3(dpa)_4Cl_2$·CH_2Cl_2.

10.1021/ja000515q CCC: $19.00
Published on Web 06/13/2000

was found that the unsymmetrical structure occurred again in yet another crystal form of **1**, namely, *u*-**1**·$Co(dpa)_2$ and also in *u*-$Co_3(dpa)_4Cl(BF_4)$, while a symmetrical structure was revealed in *s*-$Co_3(dpa)_4(BF_4)_2$.[4] More recently, we discovered that the unsymmetrical structure of **1** exists in another compound, *u*-**1**·$2CH_2Cl_2$,[5] which actually crystallized as a minor product along with the previously reported[3,4] symmetrical one, *s*-**1**·CH_2Cl_2, from the same solution. The only difference in composition for these two crystalline forms is the number of interstitial dichloromethane molecules.

Finally, a theoretical study (DFT calculations) [6] of **1** must be mentioned. The major results of this work, as reported, are as follows: (i) the ground state of the symmetric molecule has one unpaired electron, (ii) the energy of the system as a function of the position of the central cobalt atom is described by a shallow curve with a single minimum, and (iii) there are two doublet excited states lying only a few kilocalories per mole above the ground state, but (iv) no quartet state seemed to be thermally accessible. Thus, the theoretical study did not rule out, or really explain, the existence of unsymmetrical structures and the reported magnetic behavior. The authors argued against the use of the term "bond stretch isomers" that we had proposed[3,4] because they did not find an energy minimum for an asymmetric structure. However, the employment of that term had been based solely on Parkin's empirical definition[7] of it and made no reference to any theoretical concepts. Though symmetrical and unsymmetrical molecules of **1** are clearly distinguishable in the solid state, solutions made from either *s*-**1**·CH_2Cl_2 or *u*-**1**·$2CH_2Cl_2$ are identical and appear to contain symmetrical molecules.[8]

To develop a better understanding of this enigmatic molecule, we have carried out many further studies and some of the results have been published as communications.[5] Herein we present the results of a comprehensive study that involved X-ray and neutron diffraction experiments and magnetic property measurements of both isomers in the solid state.

Experimental Section

Materials. Manipulations were performed under an atmosphere of argon using standard Schlenk techniques. Solvents were purified by conventional methods and were freshly distilled under nitrogen prior to use. Anhydrous cobalt dichloride was purchased from Strem Chemicals, Inc. 2,2′-Dipyridylamine was purchased from Aldrich and sublimed prior to use. $Co_3(dpa)_4Cl_2$ was made according to a previously published procedure.[4]

Physical Measurements. IR spectra were recorded on a Perkin-Elmer 16PC FT-IR spectrometer by using KBr pellets. The SEM images were recorded on a Cameca SX50 electron microprobe (housed in the Department of Geology & Geophysics at Texas A&M University). Magnetic susceptibility measurements were obtained with the use of the following magnetometers: a Quantum Design SQUID MPMS-5 (housed in the Department of Physics and Astronomy at Michigan State University) and an MPMS-XL (housed in the Department of Chemistry at Texas A&M University). Angle rotation experiments performed on single crystals were corrected for a systematic error of the rotation system by calibration in all the principal directions. Temperature dependence studies on single crystals without the rotator system were performed by standard procedures with the crystal embedded in stopcock grease. Magnetic susceptibility data for the compound *s*-**1**·CH_2Cl_2 in the range 2−350 K at 1000 G were obtained on a finely divided polycrystalline sample (31.5 mg) and on a single crystal (27.5 mg). The data were corrected for the sample holder and for the experimental diamagnetic contribution (-7.1×10^{-4} emu mol^{-1}). This value is in good agreement with that of -5.3×10^{-4} emu mol^{-1} calculated from Pascal constants.[9] Data for *u*-**1**·$2CH_2Cl_2$ were obtained in the range 2−300 K at 1000 G on a finely divided polycrystalline sample (26 mg) and on a single crystal (10.5 mg). Higher temperatures were not accessible due to the partial loss of interstitial solvent above $T \sim 300$ K. The data were corrected for the sample holder and the diamagnetic contribution estimated from the Pascal constants[9] (-5.8×10^{-4} emu mol^{-1}). It is worthy to note that no hysteresis effect was observed in the temperature range for these experiments. EPR studies were performed on oriented single crystals on a Bruker ESP300E spectrometer equipped with an Oxford Instruments ESR900 cryostat (4.2−300 K). Elemental analyses were performed by Canadian Microanalytical Services; they were satisfactory.

Crystallization of *s*-1·CH_2Cl_2 and *u*-1·$2CH_2Cl_2$. Method A. $Co_3(dpa)_4Cl_2$ (0.48 g, 0.50 mmol) was dissolved in 20 mL of CH_2Cl_2, and 25 mL of hexanes were layered on top of the resulting solution at ambient temperature. Two types of crystals formed. Large block-shaped crystals of *s*-**1**·CH_2Cl_2 were the major component, while a small amount (∼15% of the total amount) were columnar crystals of *u*-**1**·$2CH_2Cl_2$**.** These were separated by hand for X-ray and magnetic studies.

Method B. *u*-**1**·$2CH_2Cl_2$ in higher yield was obtained by recrystallization at low temperature: *s*-**1**·CH_2Cl_2 (0.32 g, 0.30 mmol) was dissolved at room temperature in a mixture of dichloromethane (15 mL) and hexanes (5 mL). The resulting brown solution was seeded with a few small crystals of *u*-**1**·$2CH_2Cl_2$ (∼2 mg), prepared as indicated in method A. The solution was layered with hexanes (25 mL) and the mixture was cooled to 0 °C. Slow diffusion of hexanes into the solution gave crystals of *u*-**1**·$2CH_2Cl_2$ in 10 days. Yield: 0.26 g (80%). IR (KBr, cm^{-1}) for *s*-**1**·CH_2Cl_2 1606 (s), 1593 (s), 1547 (m), 1469 (s), 1459 (sh), 1424 (s), 1379 (sh), 1368 (s), 1317 (s), 1282 (m), 1269 (m), 1250 (m), 1167 (m), 1152 (s), 1116 (w), 1055 (w), 1022 (m), 884 (m), 759 (s), 748 (sh), 735 (s), 704 (sh), 648 (sh), 540 (w), 518 (w), 456 (m), 428 (m), 402 (m); IR (KBr, cm^{-1}) for *u*-**1**·$2CH_2Cl_2$ 1606 (s), 1593 (s), 1547 (m), 1468 (s), 1458 (s), 1424 (s), 1379 (sh), 1367 (m), 1313 (m), 1283 (w), 1265 (w), 1152 (m), 1108 (w), 1052 (w), 1021 (m), 1009 (sh), 887 (w), 763 (s), 747 (sh), 738 (s), 729 (s), 700 (w), 649 (w), 638 (w), 540 (w), 519 (w), 462 (w), 429 (m), 398 (m). Anal. Calcd for *s*-**1**·CH_2Cl_2 ($C_{41}H_{34}N_{12}Cl_4Co_3$): C, 48.59; H, 3.38; N, 16.59; Cl, 13.99. Found: C, 48.45; H, 3.35; N, 16.51; Cl, 14.77. Anal. Calcd for *u*-**1**·$2CH_2Cl_2$ ($C_{42}H_{36}N_{12}Cl_6Co_3$): C, 45.93; H, 3.30; N, 15.31; Cl, 19.37. Found: C, 45.38; H, 3.32; N, 15.07; Cl, 18.97. Both types of crystals seem to be indefinitely stable in air and have the same solution properties. These results have been reported elsewhere.[8]

X-ray Crystallography. In each case, a suitable crystal was attached to the end of a quartz fiber with a small amount of silicone grease and transferred to a goniometer head. Geometric and intensity data for *s*-**1**·CH_2Cl_2 were gathered at 296 K on a Nonius FAST area detector system, utilizing the program MADNES.[10] Single-crystal X-ray work at 109 K was performed on a Nonius CAD4 diffractometer. Detailed procedures have previously been described.[11]

Data collection for *u*-**1**·$2CH_2Cl_2$ was done on a Nonius FAST diffractometer at 298, 213, 173, and 133 K. The data for *u*-**1**·$2CH_2Cl_2$ at 20 K were collected on a Bruker SMART 2000 CCD detector system equipped with a liquid helium low-temperature controller.[12] Cell parameters were measured using the SMART[13] software. Data were corrected for Lorentz and polarization effects using the program SAINT.[14] Absorption corrections were applied using SADABS.[15]

(5) Cotton, F. A.; Murillo, C. A.; Wang, X. *J. Chem. Soc., Dalton Trans*. **1999**, 3327.

(6) Rohmer, M.; Bénard, M. *J. Am. Chem. Soc*. **1998**, *120*, 9372.

(7) (a) Parkin, G.; Hoffmann, R. *Angew. Chem., Int. Ed. Engl*. **1994**, *33*, 1462. (b) Parkin, G. *Chem. Rev*. **1993**, *93*, 887. (c) Parkin, G. *Acc. Chem. Res*. **1992**, *25*, 455.

(8) Cotton, F. A.; Murillo, C. A.; Wang, X. *Inorg. Chem*. **1999**, *38*, 6294.

(9) Boudreaux, E. A., Mulay, L. N., Eds. *Theory and Applications of Molecular Paramagnetism*; John Wiley & Sons: New York, 1976.

(10) Pflugrath, J.; Messerschmitt, A. *MADNES*, Munich Area Detector (New EEC) System, Version EEC 11/1/89, with enhancements by Enraf-Nonius Corp., Delft, The Netherlands. A description of MADNES appears in: Messerschmitt, A.; Pflugrath, J. *J. Appl. Crystallogr*. **1987**, *20*, 306.

(11) (a) Bryan, J. C.; Cotton, F. A.; Daniels, L. M.; Haefner, S. C.; Sattelberger, A. P. *Inorg. Chem.* **1995**, *34*, 1875. (b) Scheidt, W. R.; Turowska-Turk, I. *Inorg. Chem.* **1994**, *33*, 1314.

(12) Hardie, M. J.; Kirschbaum, K.; Martin, A.; Pinkerton, A. A. *J. Appl. Crystallogr*. **1998**, *31*, 815.

(13) SMART V5.504 Software for the CCD Detector System. Bruker Analytical Instruments Division: Madison, WI, 1998.

Table 1. Crystallographic Data for *s*-**1**·CH_2Cl_2 and *u*-**1**·$2CH_2Cl_2$

compd	*s*-**1**·CH_2Cl_2			*u*-**1**·$2CH_2Cl_2$				
formula	$C_{41}H_{34}Cl_4Co_3N_{12}$			$C_{42}H_{36}Cl_6Co_3N_{12}$				
formula wt	1013.39			1098.32				
temp, K	296(2)	109(2)	20(2)	298(2)	213(2)	173(2)	133(2)	20(2)
crystal syst	orthorhombic	monoclinic	monoclinic	tetragonal	tetragonal	tetragonal	tetragonal	tetragonal
space group	*Pnn*2	Pn	Pn	$I\bar{4}$	$I\bar{4}$	$I\bar{4}$	$I\bar{4}$	$I\bar{4}$
a, Å	12.9014(6)	11.176(2)	11.155(1)	27.378(2)	27.2558(8)	27.189(1)	27.128(1)	27.004(4)
b, Å	14.0313(6)	13.920(2)	13.923(1)	27.378(2)	27.2558(8)	27.189(1)	27.128(1)	27.004(4)
c, Å	11.2384(1)	12.740(2)	12.750(2)	12.318(1)	12.2451(7)	12.2293(7)	12.2094(9)	12.230(2)
β, deg	90	90.056(9)	90.04(1)	90	90	90	90	90
V, Å^3	2034.4(1)	1982.0(6)	1980.2(1)	9233.0(1)	9096.6(6)	9040.4(7)	8985.2(8)	8918(2)
Z	2	2	2	8	8	8	8	8
d_{calc}, g cm^{-3}	1.654	1.698	1.699	1.580	1.604	1.614	1.624	1.636
*R*1,[a] w*R*2[b] [$I > 2\sigma(I)$]	0.036, 0.090	0.031, 0.079	0.094, 0.110	0.041, 0.101	0.038, 0.091	0.038, 0.090	0.037, 0.094	0.042, 0.090
*R*1,[a] w*R*2[b] (all data)	0.038, 0.092	0.033, 0.080		0.044, 0.104	0.041, 0.093	0.040, 0.092	0.039, 0.096	0.056, 0.095
quality of fit[c]	1.097	1.097	1.17	1.077	1.136	1.022	1.084	1.055

[a] $R1 = \sum||F_o| - |F_c||\sum|F_o|$. [b] $wR_2 = [\sum[w(F_o^2 - F_c^2)^2]/\sum[w(F_o^2)^2]]^{1/2}$. [c] Quality-of-fit, based on all data. $[\sum[w(F_o^2 - F_c^2)^2]/(N_{obs} - N_{param})]^{1/2}$.

Cell parameters for FAST data were obtained from an autoindexing routine and were refined using 250 strong reflections within a 2θ range of 18.1−41.6°. Unit cell refinement for CAD4 data utilized 25 strong reflections in the 2θ range of 38.0−41.8°. Cell dimensions and Laue symmetry for all crystals were confirmed from axial photographs. All data were corrected for Lorentz and polarization effects. An empirical absorption correction based on ψ-scans was applied to the CAD4 data. Data were processed into SHELX format using the programs PROCOR[16] for those collected from the FAST diffractometer and XCAD[17] for those collected from the CAD4 diffractometer.

For all structures, some or all of the non-hydrogen atoms were found via direct methods by way of the program package SHELXTL.[18] Subsequent cycles of least-squares refinement followed by difference Fourier syntheses revealed the positions of the remaining non-hydrogen atoms. The monoclinic *Pn* form of *s*-**1**·CH_2Cl_2 at 109 K was twinned along the [100] direction with a refined ratio of twin components about 1:4. The interstitial dichloromethane molecule in the orthorhombic *Pnn*2 form of *s*-**1**·CH_2Cl_2 is disordered in two positions about a 2-fold axis. The dichloromethane molecules in *u*-**1**·$2CH_2Cl_2$ were also disordered in three positions. All hydrogen atoms were placed in idealized calculated positions in the final structural refinements. The compositions of these compounds are consistent with those obtained from elemental analysis. Other details of data collection and refinement are given in Table 1. Selected interatomic distances and angles at different temperatures for the orthorhombic and monoclinic forms of *s*-**1**·CH_2Cl_2 as well as the tetragonal form of *u*-**1**·$2CH_2Cl_2$ are provided in Tables 2, 3, and 4, respectively. Other crystallographic data are given as Supporting Information.

Neutron Data. Single-crystal time-of-flight neutron data of *u*-**1**·CH_2Cl_2 at 20 K were collected on the SCD diffractometer at the Intense Pulsed Neutron Source (IPNS) at Argonne National Laboratory. A position-sensitive area detector was used to obtain time-of-flight Laue data with a wavelength range of 0.7−4.2 Å for 36 χ and ϕ angular settings of the goniometer to cover more than one full quadrant of reciprocal space.[19] Details of the data collection and analysis procedures have been described previously.[20] A single crystal ($1.5 \times 2 \times 2$ mm^3) wrapped in aluminum foil and mounted on the tip of an aluminum pin with epoxy cement was maintained at a temperature of 20 K with a Displex closed-cycle helium refrigerator. An autoindexing routine was used to obtain an orientation matrix.[21] Integrated intensities were corrected for the Lorentz factor, the incident spectrum, and the detector efficiency. A wavelength-dependent spherical absorption correction was applied.[22] Since extinction is also strongly wavelength-dependent, symmetry-related reflections were not averaged.

The structure was refined using a locally modified version of the ORFLS programs.[23] The starting model was obtained from the X-ray structural refinement. The initial positions of the aromatic hydrogen atoms of the pyridyl groups were calculated geometrically, whereas solvent CH_2Cl_2 hydrogen atoms were located by successive difference Fourier maps derived from the neutron data. Thus, all hydrogen atoms were located and refined anisotropically. The monoclinic crystal was twinned on [100] direction, similar to that observed by X-ray analysis, with a refined ratio of twin components close to 1:2. In the final least-squares cycles, all hydrogen atoms and all CH_2Cl_2 atoms were refined with anisotropic thermal parameters. The large number of variables permitted only the positional and isotropic thermal parameters to be refined for the non-hydrogen atoms. However, the tricobalt unit was unambiguously characterized. Additional information is available as Supporting Information.

Results and Discussion

We reported earlier that compound *s*-**1**·CH_2Cl_2 crystallizes in the orthorhombic space group *Pnn*2 at 168 K.[4] As shown in Chart 1, the molecule of *s*-**1** has a symmetrical Co−Co−Co chain with a separation of 2.3178(9) Å between pairs of Co atoms and a distance of 2.520(2) Å for each of the two axial Co−Cl bonds. The metal−metal bonding in the symmetrical compound is delocalized along the linear tricobalt unit with a three-center bond order of 1.5. The symmetrical arrangement of the three Co atoms in the molecule was described as a bond stretch isomer of a different crystalline form, said to be *u*-**1**·$2CH_2Cl_2$ ·H_2O.[1] The latter compound had been obtained in very low yield (∼2%),[1] and the molecule of *u*-**1** in this peculiar compound is unsymmetrical with short, long separations of the Co atoms. A single Co−Co bond and an isolated five-coordinate Co(II) in the molecule was proposed. Despite the difference in metal-to-metal distances, other structural features are essentially the same for both compounds. Each of them consists of a linear chain of three cobalt atoms that are bridged by four dpa anions with a helical configuration. The axial coordination sites of both terminal cobalt atoms are occupied by Cl atoms.

(14) SAINT, V5.06 Software for the CCD Detector System. Bruker Analytical Instruments Division: Madison, WI, 1997.
(15) SADABS. Program for absorption correction using the Bruker CCD based on the method of: Blessing, R. H. *Acta Crystallogr.* **1995**, *A51*, 33.
(16) (a) Kabsch, W. *J. Appl. Crystallogr.* **1988**, *21*, 67. (b) Kabsch, W. *J. Appl. Crystallogr.* **1988**, *21*, 916.
(17) Harms, K. *XCAD4. Program for the reduction of CAD4 diffractometer data*. University of Marburg, Germany, 1997.
(18) SHELXTL, Version 5.03. Siemens Industrial Automation Inc., Madison, WI.
(19) Schultz, A. J. *J. Trans. Am. Crystallogr. Assoc.* **1987**, *23*, 61.
(20) Schultz, A. J.; Srinivasan, K.; Teller, R. G.; Williams, J. M.; Lukehart, C. M. *J. Am. Chem. Soc.* **1984**, *106*, 999.
(21) Jacobson, R. A. *J. Appl. Crystallogr.* **1986**, *19*, 283.
(22) Howard, J. A. K.; Johnson, O.; Schultz, A. J.; Stringer, A. M. *J. Appl. Crystallogr.* **1987**, *20*, 120.
(23) Busing, W. R.; Martin, K. O.; Levy, H. A. *ORFLS*; Report ORNL-TM-305; Oak Ridge National Laboratory, 1962.

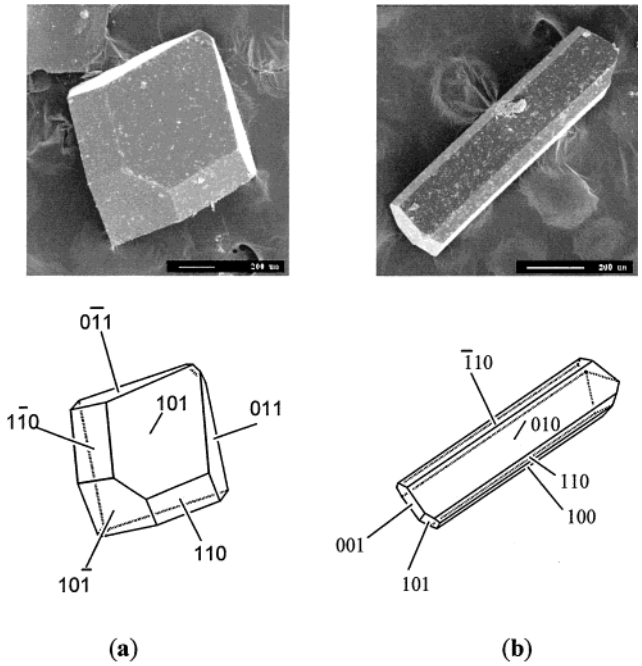

Figure 1. SEM images of two crystal forms of **1**, together with schematic drawings showing their face indices: (a) orthorhombic crystal, *s*-**1**·CH_2Cl_2; (b) tetragonal crystal, *u*-**1**·$2CH_2Cl_2$.

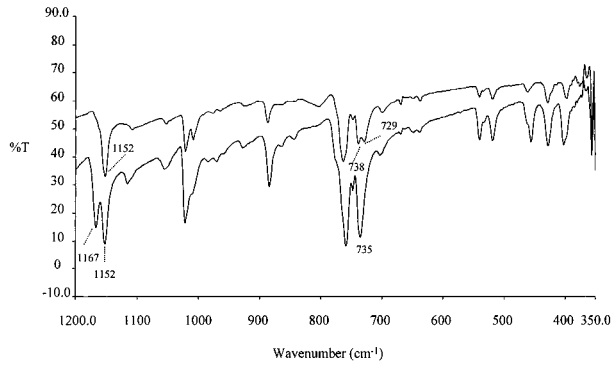

Figure 2. Comparison of the IR spectra of *s*-**1**·CH_2Cl_2 (upper) and *u*-**1**·$2CH_2Cl_2$ (lower) in the solid state.

As recently reported,[5] by careful examination of the crystals obtained by slow diffusion of hexanes into a dichloromethane solution of **1**, we found that another type of crystal with the composition *u*-**1**·$2CH_2Cl_2$ appears along with *s*-**1**·CH_2Cl_2. As shown in Figure 1, the two crystalline forms differ in their morphology with *s*-**1**·CH_2Cl_2 being block-shaped and *u*-**1**·$2CH_2Cl_2$ being columnar. Their IR spectra are essentially the same but with some interesting differences in the 1150−1170- and 700−750-cm^{-1} regions, as shown in Figure 2. The yield of the unsymmetrical form can be as high as 80% under optimized crystallization conditions as described in the Experimental Section (method B). More interestingly, *u*-**1**·$2CH_2Cl_2$ can also be prepared when pure crystals of *s*-**1**·CH_2Cl_2 are dissolved in a mixture of CH_2Cl_2/hexanes at ∼0 °C, indicating that these forms are interchangeable and the crystals they form depend only on the crystallization conditions. The amount of dichloromethane determined in the diffraction studies for *s*-**1**·CH_2Cl_2 and *u*-**1**·$2CH_2Cl_2$ is consistent with the results from elemental analysis. The existence of symmetrical and unsymmetrical molecules of **1** in these two crystalline forms has been confirmed by X-ray diffraction studies. In addition, for each of the two types of crystals there is a significant structural dependence on temperature.

Table 2. Selected Bond Lengths (Å) and Angles (deg) for the Orthorhombic Form of *s*-**1**·CH_2Cl_2 at 296 K[a]

Co(1)−Co(2)	2.3369(4)	Co(2)−Co(1A)	2.3369(4)
Co(1)−Cl(1)	2.4881(8)	Co(1)−N(4)	2.020(3)
Co(1)−N(1)	1.997(3)	Co(2)−N(5)	1.903(3)
Co(1)−N(2)	1.991(3)	Co(2)−N(6)	1.910(3)
Co(1)−N(3)	1.978(3)		
Co(1A)−Co(2)−Co(1)	177.99(5)	Co(2)−Co(1)−Cl(1)	178.86(3)
N(1)−Co(1)−N(2)	89.89(13)	N(2)−Co(1)−N(3)	171.2(1)
N(1)−Co(1)−N(3)	89.49(13)	N(2)−Co(1)−N(4)	89.8(1)
N(1)−Co(1)−N(4)	168.48(12)	N(3)−Co(1)−N(4)	89.0(1)
N(1)−Co(1)−Co(2)	84.52(8)	N(1)−Co(1)−Cl(1)	95.54(9)
N(2)−Co(1)−Co(2)	84.70(9)	N(2)−Co(1)−Cl(1)	94.16(9)
N(3)−Co(1)−Co(2)	86.45(8)	N(3)−Co(1)−Cl(1)	94.69(9)
N(4)−Co(1)−Co(2)	83.99(9)	N(4)−Co(1)−Cl(1)	95.97(9)
N(5)−Co(2)−N(6)	90.0(1)	N(6)−Co(2)−Co(1)	88.6(1)
N(5)−Co(2)−Co(1)	91.2(1)		

[a] Atoms labeled "A" are symmetry generated.

Crystal Structures. Single-crystal X-ray studies of compounds *s*-**1**·CH_2Cl_2 and *u*-**1**·$2CH_2Cl_2$ were performed in temperatures ranging from 20 to 296 K. Data for *s*-**1**·CH_2Cl_2 were obtained at 20 K by neutron diffraction.

(A) *s*-$Co_3(dpa)_4Cl_2$·CH_2Cl_2. The molecular structure of *s*-**1** in *s*-**1**·CH_2Cl_2 at 296 K is symmetrical, similar to that reported at 168 K.[3,4] The selected bond distances and angles at 296 K are listed in Table 2, and the atom labeling scheme is shown in Figure 3. Compared to the data obtained at 168 K, there are very small changes of the interatomic distances. The Co(1)−Co(2) distance of 2.3369(4) Å at 296 K is ∼0.019 Å longer, and the Co(1)−Cl(1) distance of 2.4881(8) Å is ∼0.032 Å shorter. Although the cobalt-containing molecule of *s*-**1** is well-defined, the interstitial dichloromethane molecule was found to be disordered on two positions related by a crystallographic 2-fold axis.

Just below 168 K, single crystals of *s*-**1**·CH_2Cl_2 undergo a phase transition from an orthorhombic form to a monoclinic form. The phase transition is evidenced by the appearance of diffraction intensities of 0*k*0 reflections with $k = 2n + 1$ as the temperature is lowered. These reflections should be absent for space group *Pnn*2, and their appearance shows that the crystal has been transformed to the monoclinic space group *Pn* (which is a subgroup of the orthorhombic *Pnn*2 group). The X-ray structure obtained at 109 K shows that the entire molecule of *s*-**1** is on a general position with no crystallographic symmetry imposed (Figure 4). At this temperature, the crystal appears, superficially, to be orthorhombic because the β-angle is nearly 90°, but close examination of the data indicates that the low-temperature phase is twinned about the monoclinic *a* axis. There are probably domains in which the distortion is in one direction [100] during the cooling process, and other domains in which it is in the opposite direction [$\bar{1}$00]. Selected interatomic distances and angles for the monoclinic structure are listed in Table 3. The two independent metal−metal distances, 2.3224(8) and 2.3214(8) Å, remain the same within the experimental error. The pseudo-D_4 point group symmetry of the molecule remains at lower temperature, even though a phase transition has occurred.

There are two questions raised at this stage. First, what is the cause of the phase change? Second, what kind of phase transition is it? These questions were answered by detailed neutron diffraction studies.

The neutron data were collected at 20 K, using the time-of-flight Laue technique.[19,20] The neutron data allowed successful refinement of the structure in space group *Pn* to give a symmetrical molecular structure of *s*-**1**, which is essentially the same as that obtained from X-ray diffraction study at 109 K

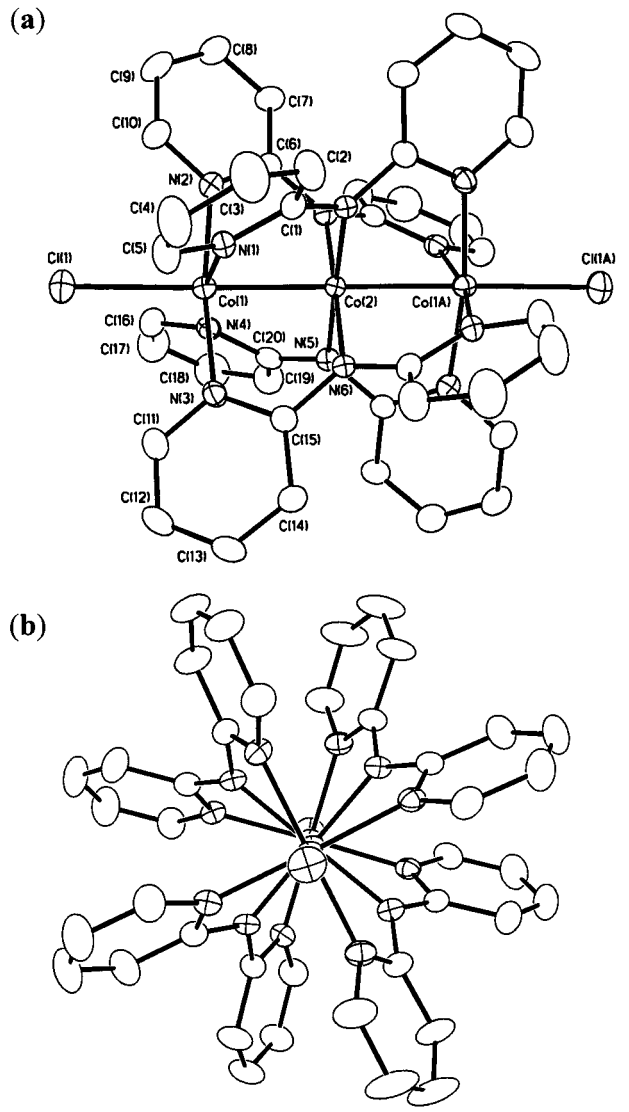

Figure 3. (a) Perspective view of the molecule of *s*-**1** in s-**1**·CH_2Cl_2 at 296 K. Atoms are drawn at their 40% probability levels. Hydrogen atoms are omitted for clarity. (b) A view of the molecule of *s*-**1** looking down the Co_3 axis.

(Figure 4). The resulting interatomic distances and angles are listed in Table 3. A remarkable feature of the *Pn* structure is that the solvent molecule CH_2Cl_2 becomes well ordered. All hydrogen atoms in the structure were refined anisotropically by using the neutron data. As shown in Figure 5a, one of the axial Cl atoms is involved in hydrogen bonding with the ordered solvent molecule in the solid state. The Cl(2)···H(41A) distance of 2.635(7) Å is indicative of a very weak hydrogen-bonding interaction. Atom Cl(1) on the other end is more than 3.0 Å away from the CH_2Cl_2 molecule. The solvent molecule is disordered in the higher temperature *Pnn*2 phase. A drawing of the CH_2Cl_2 molecule at 296 K is presented in Figure 5b for comparison. It seems that a displacive ordering of the solvent molecule at lower temperature leads to a phase transition. Despite this, the molecules of *s*-**1** remain essentially, if not rigorously, symmetrical throughout the temperature range 20−296 K.

Further insight into the phase transition process of *s*-**1**·CH_2Cl_2 was achieved by monitoring the change of neutron diffraction intensities of *0k*0 reflections in the temperature range 20−250 K. The results are shown in Figure 6. The intensity of the 0*7*0 reflection (inset of Figure 6) at various temperatures is

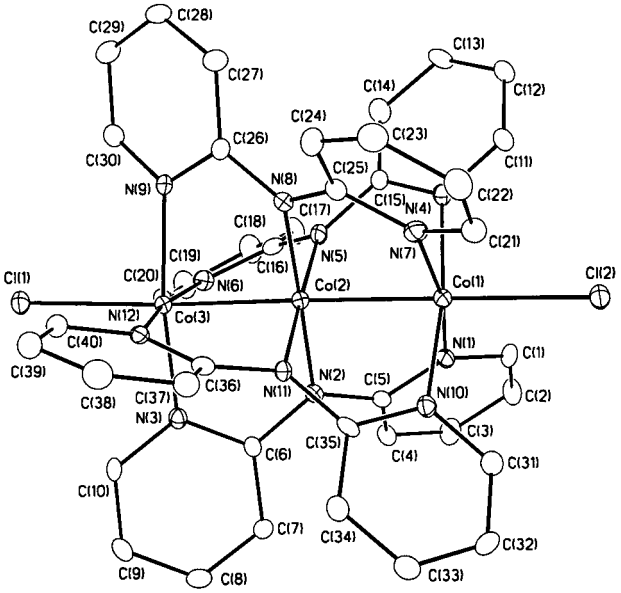

Figure 4. Perspective view of the molecule of *s*-**1** in *s*-**1**·CH_2Cl_2 at 109 K. Atoms are drawn at their 40% probability levels. Hydrogen atoms are omitted for clarity.

directly proportional to the square of the order parameter defined by an Ising model.[24] This feature allows us to conclude that the displacive transition occurs around 165 K. As previously described, this second-order phase transition is associated with the ordering of the solvent molecules and their hydrogen-bonding interactions.

A plot of selected interatomic distances versus temperature for *s*-**1**·CH_2Cl_2 is shown in Figure 7. There are substantial variations of chloride-to-terminal cobalt distances at low temperature. The two equal Co−Cl distances of 2.4881(8) Å at 296 K change to 2.508(7) and 2.445(7) Å at 20 K. The two chloride ions are not equivalent because only one of them, Cl(2), is involved in a hydrogen-bonding interaction with the CH_2Cl_2 molecule in the monoclinic phase; this leads to weaker Co−Cl bonding and a longer Co−Cl distance. No other distinct differences in the remaining interatomic distances and angles at low temperature are observed. The mean Co−N distance for the central atom Co(2) changes from 1.907 to 1.904 Å, while the average terminal Co−N distance decreases from 1.997 to 1.974 Å. Most importantly, the three cobalt atoms are arranged essentially symmetrically and the metal−metal distances remain essentially constant at all temperatures (Figure 7a).

(B) *u*-$Co_3(dpa)_4Cl_2$·$2CH_2Cl_2$. The tetragonal crystals of *u*-**1**·$2CH_2Cl_2$ were isolated from the same mother liquor containing *s*-**1**·CH_2Cl_2. The crystal structure of *u*-**1**·$2CH_2Cl_2$ was studied at temperatures of 298, 213, 173, 133, and 20 K. The tetragonal symmetry and $I\bar{4}$ space group of the crystal is maintained at all these temperatures. Selected interatomic distances and angles are listed in Table 4. The molecule of *u*-**1** lies on a general position. The three linear Co atoms are arranged unsymmetrically as shown in Figure 8. The short and long separations of the Co atoms at 298 K are 2.299(1) and 2.471(1) Å, respectively. The short Co(1)−Co(2) distance is comparable to those of dinuclear cobalt compounds, in which a single Co−Co bond exists.[2] The third atom, Co(3), which is not bonded to the central atom Co(2), is coordinated by four pyridyl N atoms and a Cl^-

(24) (a) Ravy, S. Ph.D. Dissertation, Paris-Sud Centre d'Orsay University, 1988. (b) and Pouget, J. P. In *Low dimensional conductors and superconductors*; Jérome, D., Caron, L. G., Eds.; NATO ASI Ser. B Plenum Press: New York, 1987; Vol. 155, pp 17−45. (c) Kagoshima, S.; Ishiguro, T.; Schultz, T. D.; Tomkiewicz, Y. *Solid State Commun.* **1978**, *28*, 485.

Table 3. Selected Bond Lengths (Å) and Angles (deg) for the Monoclinic Form of *s*-**1**·CH_2Cl_2 at 109 and 20 K

	109 K	20 K
Co(1)−Co(2)	2.3224(8)	2.34(1)
Co(2)−Co(3)	2.3214(8)	2.34(1)
Co(1)−Cl(2)	2.499(1)	2.508(7)
Co(3)−Cl(1)	2.476(1)	2.445(7)
Co(1)−N(1)	1.967(4)	1.978(6)
Co(1)−N(4)	1.970(4)	1.954(6)
Co(1)−N(7)	2.007(4)	2.009(6)
Co(1)−N(10)	1.978(4)	1.982(6)
Co(2)−N(2)	1.906(4)	1.905(7)
Co(2)−N(5)	1.902(4)	1.917(7)
Co(2)−N(8)	1.894(4)	1.895(7)
Co(2)−N(11)	1.901(4)	1.898(7)
Co(3)−N(3)	1.942(4)	1.947(6)
Co(3)−N(6)	1.963(4)	1.964(6)
Co(3)−N(9)	1.984(4)	1.985(6)
Co(3)−N(12)	2.022(4)	2.050(6)
Co(1)−Co(2)−Co(3)	176.51(4)	175.8(3)
Co(2)−Co(3)−Cl(1)	177.27(4)	177.1(3)
Co(2)−Co(1)−Cl(2)	178.84(4)	178.3(3)
N(1)−Co(1)−N(4)	90.1(2)	90.6(2)
N(1)−Co(1)−N(7)	169.6(2)	169.7(4)
N(1)−Co(1)−N(10)	90.2(2)	89.9(3)
N(4)−Co(1)−N(7)	89.9(2)	89.7(2)
N(4)−Co(1)−N(10)	172.3(2)	172.4(4)
N(7)−Co(1)−N(10)	88.5(2)	88.4(2)
N(1)−Co(1)−Cl(2)	95.0(1)	94.9(2)
N(4)−Co(1)−Cl(2)	93.9(1)	93.9(3)
N(7)−Co(1)−Cl(2)	95.4(1)	95.3(2)
N(10)−Co(1)−Cl(2)	93.7(1)	93.5(2)
N(2)−Co(2)−N(5)	90.6(2)	90.6(2)
N(2)−Co(2)−N(8)	178.7(2)	179.2(4)
N(2)−Co(2)−N(11)	89.8(2)	90.0(3)
N(5)−Co(2)−N(8)	90.3(2)	90.1(3)
N(5)−Co(2)−N(11)	178.4(2)	177.3(5)
N(8)−Co(2)−N(11)	89.4(2)	89.3(2)
N(3)−Co(3)−N(6)	90.1(2)	90.0(3)
N(3)−Co(3)−N(9)	172.0(2)	170.0(4)
N(6)−Co(3)−N(9)	89.4(2)	87.4(2)
N(3)−Co(3)−N(12)	88.0(2)	89.8(3)
N(6)−Co(3)−N(12)	169.6(2)	168.0(4)
N(9)−Co(3)−N(12)	91.0(2)	90.8(2)
N(3)−Co(3)−Cl(1)	95.0(1)	95.6(3)
N(6)−Co(3)−Cl(1)	94.9(1)	96.4(2)
N(9)−Co(3)−Cl(1)	93.0(1)	94.3(2)
N(12)−Co(3)−Cl(1)	95.4(1)	95.4(3)

ion and resides in a square pyramidal environment. At 298 K, the cobalt atom lies 0.327(2) Å out of the basal plane defined by atoms N(3), N(6), N(9), and N(10). The Co(3)-to-basal N distances of 2.100−2.137 Å are considerably longer than those for the metal−metal bonded Co(1) and Co(2) atoms in *u*-**1**, which are in the range 1.905−1.990 Å. The long Co(3)−N distances are similar to those observed in high-spin five-coordinate Co(II) complexes.[25] It should be pointed out that the Co(3)−Cl(2) distance of 2.363(2) Å is shorter than the Co(1)−Cl(1) distance of 2.434(2) Å, which indicates that the weaker Co−N bonding around the Co(3) atom is compensated by a stronger Co−Cl interaction. Similar results have also been reported for the other two unsymmetrical tricobalt complexes, $Co_3(dpa)_4Cl_2$·$Co(dpa)_2$ and $Co_3(dpa)_4Cl(BF_4)$·$2CH_2Cl_2$.[4]

The tetragonal form *u*-**1**·$2CH_2Cl_2$ characterized here is isomorphous with the trinickel compound $Ni_3(dpa)_4Cl_2$·$2CH_2Cl_2$, but the latter has a very nearly, though not rigorously symmetrical arrangement of three nickel atoms.[26] Compound *u*-**1**·$2CH_2Cl_2$ has unit cell dimensions (Table 1) very similar to the previously reported **1**·$2CH_2Cl_2$·H_2O,[1] thus raising a question as to whether H_2O is actually present, as reported.

The fact that *u*-**1**·$2CH_2Cl_2$ crystallizes along with *s*-**1**·CH_2Cl_2 from the same solution and that there is only one Co−Co bond between two Co atoms in the former but a delocalized bond exists over three Co atoms in the latter compound justifies the statement that they indeed represent a pair of "bond stretch isomers". It is important to note that the symmetrical and unsymmetrical forms of **1** do not interconvert in the solid state. Instead, they retain distinctive structural and physical properties at all temperatures. While a phase transition has been observed for the orthorhombic crystals, the linear tricobalt moiety remains essentially symmetrical at all temperatures. For the tetragonal crystals of *u*-**1**·$2CH_2Cl_2$, the space group does not change with temperature, although the five-coordinate Co atom in the unsymmetric molecule of *u*-**1** experiences significant variations in interatomic distances and angles at different temperatures.

Plots of the temperature dependence of selected interatomic distances for *u*-**1**·$2CH_2Cl_2$ are shown in Figure 9. The interatomic distances (Co−Co and Co−N) in the metal−metal bonded Co(1)−Co(2) unit remain essentially the same from 298 to 20 K (the changes are less than 0.01 Å). In contrast, distances involving the five-coordinate Co(3) atom, which is in a square pyramidal environment, change significantly. At 20 K, the Co(3)−N distances are 0.075 to 0.084 Å shorter than they are at 298 K, and the Co(3)−Co(2) separation is also shortened by 0.086 Å. A comparison of coordination geometry for atom Co(3) at temperatures 298 and 20 K is shown in Figure 10. The distance between atom Co(3) and the centroid of the basal plane decreases from 0.327(2) Å to 0.221(1) Å, a total change of 0.106 Å from 298 to 20 K, whereas the Co(3)−Cl(2) distance increases by 0.077 Å. The shift of Co(3) also leads to shortening of the Co(3)−Co(2) distance by 0.086 Å. Consequently, the unsymmetrical short and long Co−Co distances of 2.299(1) and 2.471(1) Å at room temperature change to 2.3035(7) and 2.3847(8) Å at 20 K. The molecule of *u*-**1** in *u*-**1**·$2CH_2Cl_2$ becomes more symmetrical at low temperature, but the distance of ∼2.38 Å between the cobalt atoms is still significantly longer than those observed for dinuclear compounds with a Co−Co single bond.[2] On the basis of the observed distances and angles, it is reasonable to suggest that at low temperature the Co(3) atom is in a five-coordinate environment with a low-spin state.

Magnetic and EPR Measurements. (A) *s*-$Co_3(dpa)_4Cl_2$·CH_2Cl_2. Compounds *s*-**1**·CH_2Cl_2 and *u*-**1**·$2CH_2Cl_2$ exhibit different magnetic behavior in the solid state. Figure 11 shows the temperature dependence of the measured effective magnetic moment μ_{eff} for a polycrystalline sample of *s*-**1**·CH_2Cl_2 (the crystals were previously tested by X-ray diffraction and then finely ground). It displays a plateau at 2.07 μ_B between 8 and 160 K which indicates the existence of a doublet ground state ($S = {}^1/_2$) with a *g* factor of 2.38(2). This is supported by the field dependence of the magnetization, which can be fitted by the Brillouin function for an $S = {}^1/_2$ with a *g* factor around 2.35(2). Below 8 K, the slight decrease of the μ_{eff} is attributed to the onset of weak antiferromagnetic interactions between trinuclear molecules ($|J| < 0.5$ K).

To determine the *g* tensor more accurately, we measured the EPR spectra on an oriented single crystal of *s*-**1**·CH_2Cl_2. At

(25) (a) Boca, R.; Elias, H.; Haase, W.; Hüber, M.; Klement, R.; Müller, L.; Paulus, H.; Svoboda, I.; Valko, M. *Inorg. Chim. Acta* **1998**, *278*, 127. (b) Utsuno, S.; Ando, T.; Ishida, M. *J. Coord. Chem.* **1996**, *38*, 29. (c) Drabent, K.; Wolny, J. A.; Chmielewski, P. J.; Gatner, K.; Rudolf, M. F. *Polyhedron* **1993**, *12*, 651. (d) Kennedy, B. J.; Fallon, G. D.; Gatehouse, B. M. K. C.; Murray, K. S. *Inorg. Chem.* **1984**, *23*, 580. (e) Calligaris, M.; Nardin, G.; Randaccio, L. *J. Chem. Soc., Dalton Trans.* **1974**, 1903. (f) Orlandini, A. B.; Calabresi, C.; Ghilardi, C. A.; Orioli. P. L.; Sacconi, L. *J. Chem. Soc., Dalton Trans.* **1973**, 1383. (g) Calligaris, M.; Minichelli, D.; Nardin, G.; Randaccio, L. *J. Chem. Soc. A* **1970**, 2411.

(26) Clérac, R.; Cotton, F. A.; Dunbar, K. R.; Murillo, C. A.; Pascual, I.; Wang, X. *Inorg. Chem.* **1999**, *38*, 2655.

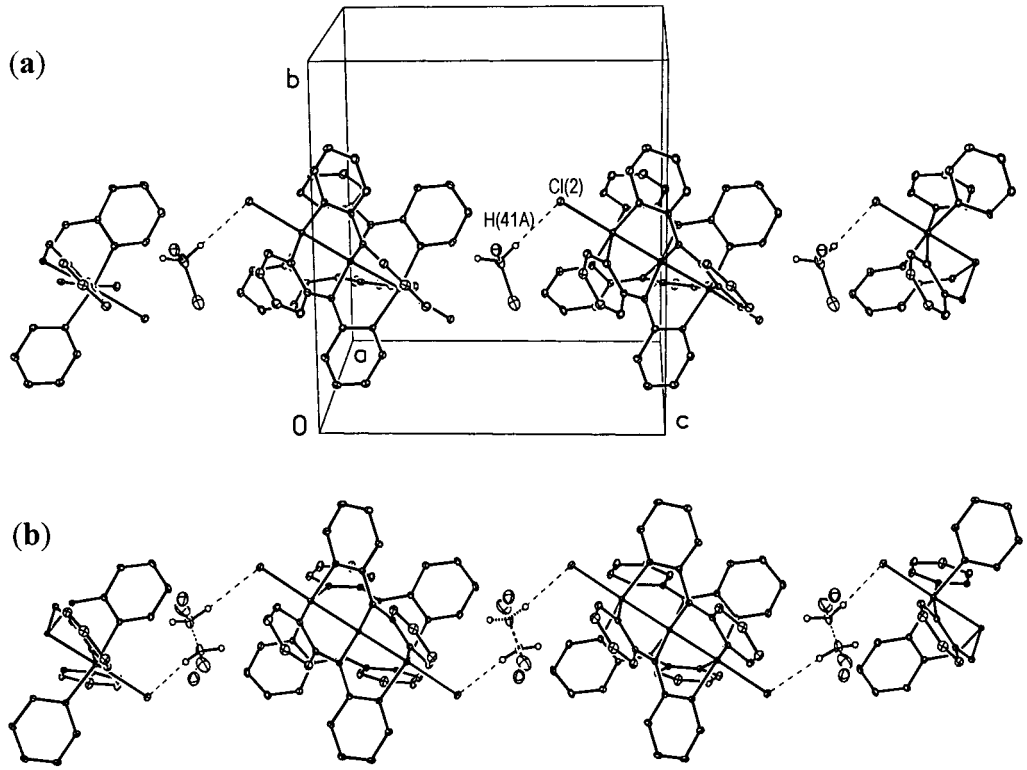

Figure 5. (a) A drawing of the extended structure of the monoclinic crystal of *s*-**1**·CH_2Cl_2 along the *bc* plane at 20 K. Atom Cl(2) is hydrogen-bonded to an interstitial dichloromethane molecule with a Cl(2)−H(41A) distance of 2.635(7) Å. (b) A drawing of the extended structure of the orthorhombic crystal of *s*-**1**·CH_2Cl_2 at 296 K. The interstitial dichloromethane molecules are disordered in two positions.

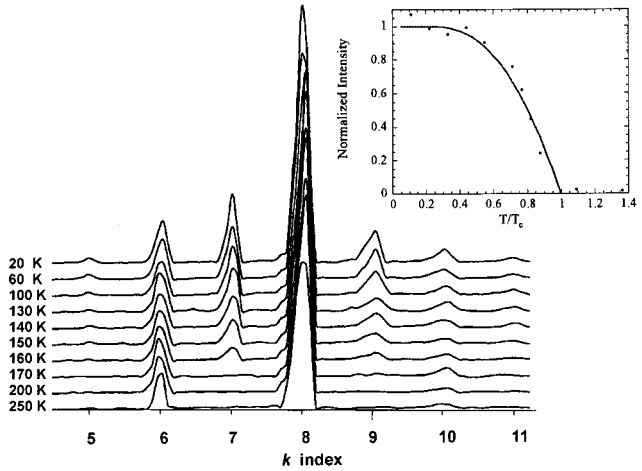

Figure 6. Plot of neutron diffraction intensities for 0*k*0 reflections in space group *Pnn*2 versus temperature for *s*-**1**·CH_2Cl_2. Systematic absence violations for reflections 0*k*0, where $k = 3, 7, 9, 11$, at low temperature is consistent with a phase transition to monoclinic *Pn* symmetry. Inset: thermal variation of the normalized intensity of the 070 reflection; the black line is the fitting obtained with an Ising model.

room temperature, *s*-**1**·CH_2Cl_2 is EPR silent for all crystal orientations. Below 200 K, a resonance with a line width of $\Delta H \approx 4000$ G appears in the *a* direction which become more symmetrical and narrower with decreasing temperatures. A *g* value of ~2.40(1) was obtained at 80 K (Figure 12 inset). At 4.2 K, a sharper Lorentzian line ($120 < \Delta H < 240$ G) is observed in all the directions (Figure 12). The eigenvalues of *g* coincide with the crystallographic axes as expected for pseudo-orthorhombic symmetry.[27] The values are $g_a = 2.362(5)$, $g_b = 2.317(5)$, and $g_c = 2.216(5)$ (where *a*, *b*, and *c* are the unit cell axes at room temperature) and $g_{av} = 2.298(5)$. These values are in good agreement with those reported in solution[8] and with the one estimated from the magnetic susceptibility studies on a powder sample of *s*-**1**·CH_2Cl_2 (at 4.2 K, $\mu_{eff} = 2.01\ \mu_B$, $g = 2.32(2)$). Other compounds in this family also exhibit similar *g* values.[28] The single-crystal susceptibility measurements show a very small difference (shift) and exactly the same shape of the curve of the effective moment versus temperature as that observed for the powder sample. This result is easily explained by the small anisotropy of the *g* factor found by EPR and a small thermal variation of the *g* tensor expected by the almost temperature-independent molecular structure of *s*-**1** (Figure 7). From the crystal structure (one orientation of the *s*-**1** molecule) and the eigenvalues of *g* determined by EPR experiments on a single crystal at 4.2 K, the *g* tensor of the *s*-**1** molecule is found to be $g_{||} = 2.163(5)$ and $g_{\perp} = 2.363(5)$. A listing of the *g* tensors is found in Table 5.

At temperatures between 160 and 350 K, μ_{eff} increases gradually in a manner typical for a spin crossover process. Such behavior has been observed in other compounds of this family.[8,28] The lack of saturation at 350 K (which is the highest temperature one can achieve without loss of crystal integrity) renders it difficult to assign a value for the high-spin state. Nevertheless, we have attempted to help resolve this issue by examining the corresponding properties of [*s*-**1**]$^+$. Our earlier finding that the oxidized compound exhibits an unprecedented two-step spin crossover from $S = 0$ to $S = 1$ and then $S = 1$ to $S = 2$[28a] suggests that the high-spin state for *s*-**1** is either $S = {}^3/_2$ or $S = {}^5/_2$. A ideal solution model for an $S = {}^1/_2 \leftrightarrow S = {}^3/_2$ or an $S = {}^1/_2 \leftrightarrow S = {}^5/_2$ spin crossover has been used to fit the magnetic data, the results of which are depicted in Figure 11b and c.[29] The derived enthalpy and entropy variations associated

(27) Landau, L.; Lifchitz, E. *Elasticity Theory*; Mir: Moscow, 1967.

(28) (a) Clérac, R.; Cotton, F. A.; Dunbar, K. R.; Lu, T.; Murillo, C. A.; Wang, X. *J. Am. Chem. Soc.* **2000**, *122*, 2272. (b) Clérac, R.; Cotton, F. A.; Dunbar, K. R.; Lu, T.; Murillo, C. A.; Wang, X. *Inorg. Chem.*, in press.

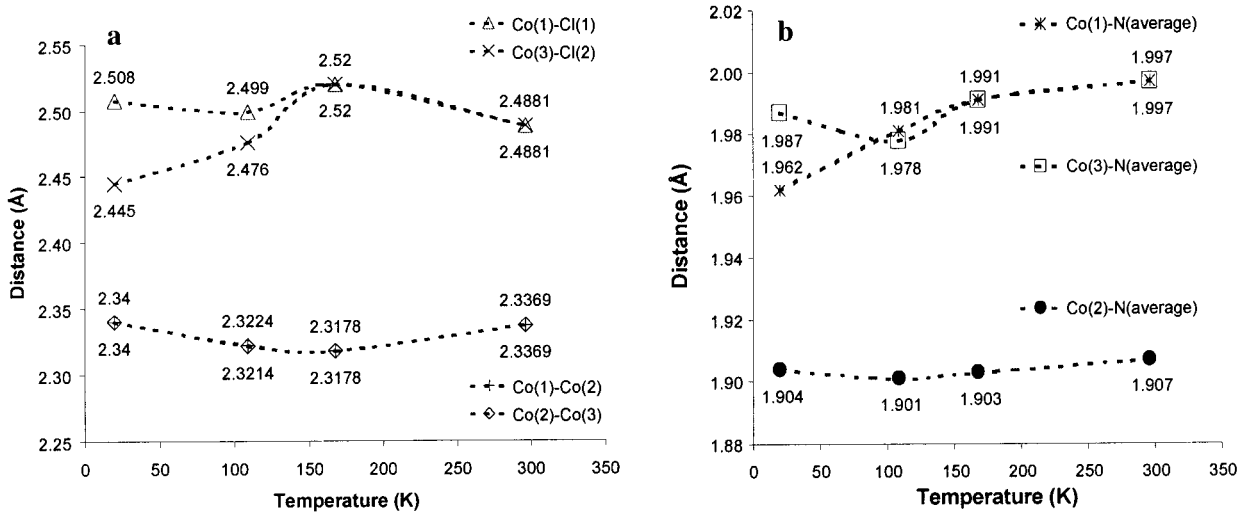

Figure 7. Temperature dependence of selected interatomic distances for *s*-**1**·CH_2Cl_2.

Table 4. Selected Bond Lengths (Å) and Angles (deg) for the Tetragonal Form of *u*-**1**·$2CH_2Cl_2$ at Various Temperatures

	298 K	213 K	173 K	133 K	20 K
Co(1)−Co(2)	2.299(1)	2.2943(9)	2.2958(9)	2.295(1)	2.3035(7)
Co(2)−Co(3)	2.471(1)	2.466(1)	2.457(1)	2.440(1)	2.3847(8)
Co(1)−Cl(1)	2.434(2)	2.432(1)	2.429(2)	2.427(2)	2.428(1)
Co(3)−Cl(2)	2.363(2)	2.369(2)	2.380(2)	2.391(2)	2.440(1)
Co(1)−N(1)	1.973(5)	1.973(5)	1.972(4)	1.974(4)	1.975(3)
Co(1)−N(4)	1.972(5)	1.970(5)	1.975(4)	1.966(4)	1.975(2)
Co(1)−N(7)	1.978(5)	1.975(4)	1.975(4)	1.974(4)	1.974(3)
Co(1)−N(12)	1.990(5)	1.978(4)	1.980(4)	1.980(4)	1.987(3)
Co(2)−N(2)	1.912(4)	1.904(4)	1.902(4)	1.890(4)	1.897(2)
Co(2)−N(5)	1.908(5)	1.900(4)	1.901(4)	1.903(4)	1.901(2)
Co(2)−N(8)	1.905(5)	1.909(4)	1.910(4)	1.908(4)	1.907(2)
Co(2)−N(11)	1.913(4)	1.910(4)	1.909(4)	1.908(4)	1.899(2)
Co(3)−N(3)	2.126(5)	2.124(5)	2.116(4)	2.102(4)	2.049(3)
Co(3)−N(6)	2.137(5)	2.131(5)	2.125(4)	2.104(4)	2.057(3)
Co(3)−N(9)	2.100(5)	2.099(4)	2.082(4)	2.069(4)	2.016(3)
Co(3)−N(10)	2.114(5)	2.107(5)	2.101(5)	2.093(4)	2.039(3)
Co(1)−Co(2)−Co(3)	178.00(4)	177.74(4)	177.67(4)	177.60(4)	177.46(3)
Cl(1)−Co(1)−Co(2)	179.50(5)	179.54(5)	179.54(5)	179.40(5)	179.19(3)
Cl(2)−Co(3)−Co(2)	178.60(6)	178.55(5)	178.55(5)	178.43(5)	177.80(3)
N(1)−Co(1)−N(4)	90.6(2)	90.4(2)	90.2(2)	90.2(2)	90.1(1)
N(1)−Co(1)−N(7)	171.4(2)	171.8(2)	171.6(2)	171.8(2)	171.1(1)
N(1)−Co(1)−N(12)	89.4(2)	89.7(2)	89.6(2)	89.6(2)	89.9(1)
N(4)−Co(1)−N(7)	88.7(2)	88.5(2)	88.7(2)	88.8(2)	88.6(1)
N(4)−Co(1)−N(12)	170.2(2)	170.7(2)	170.8(2)	170.8(2)	170.4(1)
N(7)−Co(1)−N(12)	89.8(2)	90.2(2)	90.1(2)	90.1(2)	90.0(1)
N(1)−Co(1)−Cl(1)	94.2(1)	94.0(1)	94.1(1)	94.0(1)	94.13(9)
N(4)−Co(1)−Cl(1)	95.3(2)	95.1(1)	95.2(1)	95.1(1)	95.07(9)
N(7)−Co(1)−Cl(1)	94.5(2)	94.2(1)	94.3(1)	94.3(1)	94.71(9)
N(12)−Co(1)−Cl(1)	94.5(2)	94.1(1)	94.1(1)	94.1(1)	94.54(9)
N(2)−Co(2)−N(5)	90.4(2)	90.5(2)	90.6(2)	90.5(2)	90.5(1)
N(2)−Co(2)−N(8)	178.7(2)	179.0(2)	178.9(2)	179.0(2)	179.3(1)
N(2)−Co(2)−N(11)	90.1(2)	90.1(2)	90.1(2)	90.1(2)	89.4(1)
N(5)−Co(2)−N(8)	89.9(2)	89.8(2)	89.8(2)	89.8(2)	89.8(1)
N(5)−Co(2)−N(11)	179.0(2)	179.2(2)	179.1(2)	179.2(2)	179.1(1)
N(8)−Co(2)−N(11)	89.5(2)	89.6(2)	89.5(2)	89.6(2)	89.4(1)
N(3)−Co(3)−N(6)	89.8(2)	89.6(2)	89.8(2)	90.1(2)	90.7(1)
N(3)−Co(3)−N(9)	161.1(2)	161.5(2)	162.1(2)	163.0(2)	166.8(1)
N(3)−Co(3)−N(10)	91.8(2)	91.7(2)	91.8(2)	91.8(2)	91.6(1)
N(6)−Co(3)−N(9)	84.1(2)	84.2(2)	83.9(2)	84.4(2)	85.3(1)
N(6)−Co(3)−N(10)	162.6(2)	163.2(2)	163.5(2)	164.6(2)	167.4(1)
N(9)−Co(3)−N(10)	88.9(2)	89.4(2)	89.6(2)	89.4(2)	89.7(1)
N(3)−Co(3)−Cl(2)	98.3(1)	98.1(1)	97.9(1)	97.6(1)	95.92(9)
N(6)−Co(3)−Cl(2)	99.3(1)	98.9(1)	98.7(1)	98.2(1)	97.16(9)
N(9)−Co(3)−Cl(2)	100.3(1)	100.1(1)	99.6(1)	99.2(1)	97.06(9)
N(10)−Co(3)−Cl(2)	97.7(1)	97.5(1)	97.3(1)	96.7(1)	94.88(9)

with the two possible types of spin crossover process listed in Table 6 are in the range of those reported for other Co^{II} spin crossover complexes.[30] As is evident in the curve fitting (Figure 11b and c), the $S = {}^1/_2 \leftrightarrow S = {}^5/_2$ model is the best. It should be pointed out, however, that the lack of saturation of μ_{eff} at high temperature makes the fitting more susceptible to slight changes in *g* value with temperature and to small experimental errors.

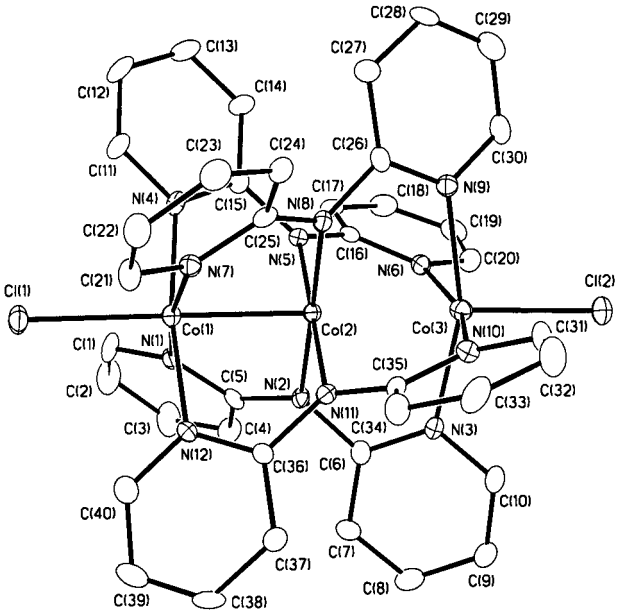

Figure 8. Perspective view of the molecule of *u*-**1** in *u*-**1**·$2CH_2Cl_2$ at 213 K. Atoms are drawn at their 40% probability levels. Hydrogen atoms are omitted for clarity.

(B) *u*-$Co_3(dpa)_4Cl_2$·$2CH_2Cl_2$. Magnetic studies of *u*-**1**·$2CH_2Cl_2$ also revealed a spin crossover behavior similar to that for *s*-**1**·CH_2Cl_2, but the temperature dependence of μ_{eff} is different from what has been observed for other members of this family.[28] As shown in Figure 13, the polycrystalline sample of *u*-**1**·$2CH_2Cl_2$ exhibits a spin crossover process. From 10 to 300 K, μ_{eff}

(29) The ideal solution model for a spin equilibrium process is described in ref 30. The equation used is given below:

$$\chi T = \frac{(\chi T_{HS} - \chi T_{LS})}{1 + \exp\left(\frac{\Delta H}{R}\left(\frac{1}{T} - \frac{1}{T_{sc}}\right)\right)} + \chi T_{LS}$$

We postulated that the *g* factor was constant at 2.35 in all the range of temperatures studied. This is expected by a comparison of magnetic susceptibility measurements on powder and single-crystal samples of *s*-**1**·CH_2Cl_2 and also by an absence of structural change with temperature.

(30) Kahn, O.*Molecular Magnetism;* VCH Publishers: New York, 1993; p 59.

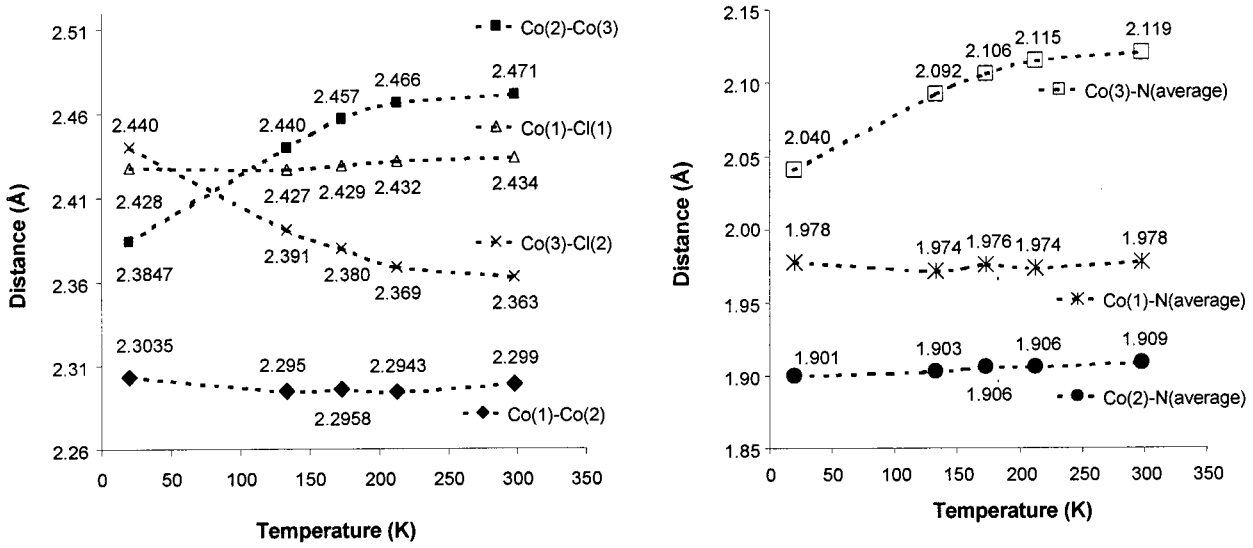

Figure 9. Temperature dependence of selected interatomic distances for *u*-**1**·$2CH_2Cl_2$.

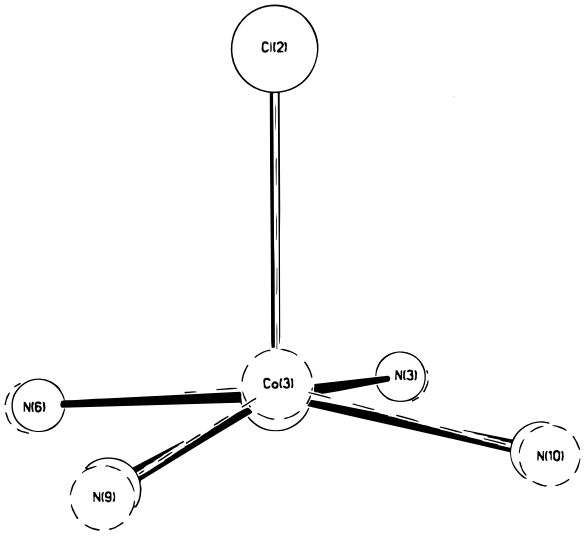

Figure 10. Plot of the coordination geometry of Co(3) for *u*-**1** at temperatures 298 (dashed lines) and 20 K (solid lines). The five-coordinate Co(3) atom is shifted toward the plane defined by atoms {N(3), N(6), N(9), N(10)}at lower temperature.

increases from 2.90 to 4.47 μ_B with the typical "S"-shaped curve of a spin crossover process, but there is no plateau showing a stable spin state in either the high- or low-temperature regimes. The moment of 2.85 μ_B at 10 K is high compare to the spin-only value expected for a $S = {}^1/_2$ ground state. To obtain more information on this intriguing behavior, magnetic susceptibility data were measured on a single crystal of *u*-**1**·$2CH_2Cl_2$. The angular dependence of the susceptibility in the principal planes at 300 and 10 K is shown in Figure 13b. The effective magnetic moment in the *ab* plane is isotropic, in accord with the tetragonal symmetry of the crystal.[27] A high degree of magnetic anisotropy was observed for the single crystal between the Δ axis (being an arbitrary axis in the isotropic *ab* plane) and the *c* axis with $(\mu_{eff})_\Delta = 3.24\ \mu_B$ and $(\mu_{eff})_c = 1.96\ \mu_B$ at 10 K. These values increased to 4.86 and 3.42 μ_B at 300 K. The thermal dependence of μ_{eff} along the Δ and *c* axes are displayed in Figure 13a. Note that these curves are qualitatively similar to the spin crossover behavior found for the powder sample. As expected for tetragonal symmetry, the susceptibility measured on a powder sample is very close to the one calculated from the single-crystal

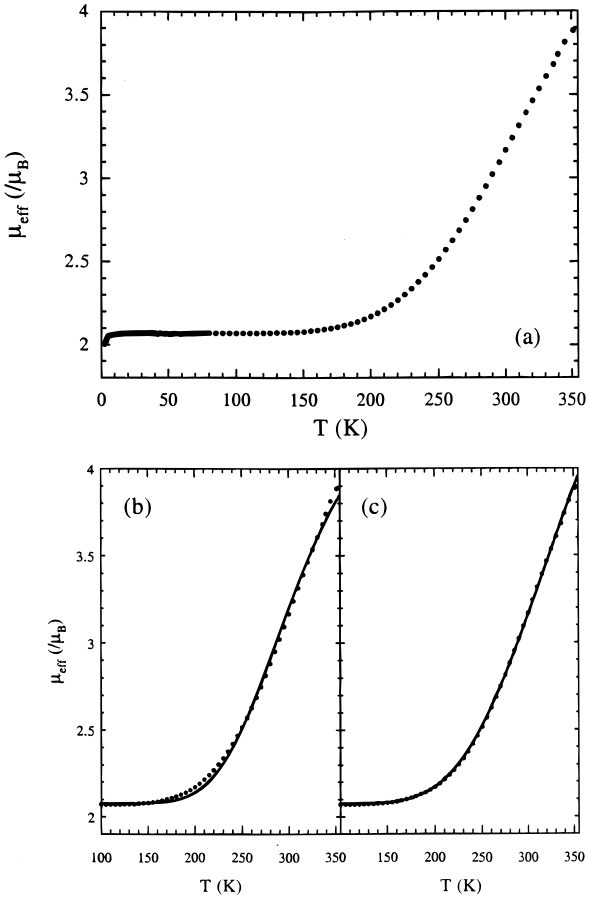

Figure 11. Temperature dependence of the magnetic effective moment for *s*-**1**·CH_2Cl_2: (a) in the whole range of temperature; (b) and (c) fitting of the experimental data by an ideal solution model of spin crossover for $S = {}^1/_2$ to $S = {}^3/_2$ and $S = {}^1/_2$ to $S = {}^5/_2$, respectively.

experiments (solid line in Figure 13a) following the relationship

$$\chi = \frac{1}{3}(2\chi_\perp + \chi_{||}) \qquad (1)$$

where χ is the magnetic susceptibility and $\mu_{eff} = (8\chi T)^{1/2}\ \mu_B$. This observation also underscores the reproducibility of the measurements.

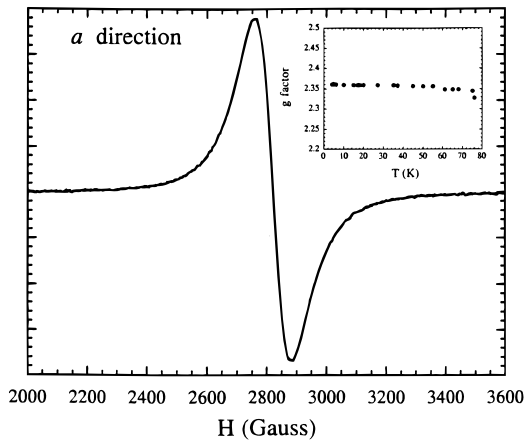

Figure 12. X-band EPR spectrum at 4.2 K on a single crystal of *s*-**1**·CH_2Cl_2 in the *a* direction. Inset: temperature dependence (below 80 K) of the *g* factor measured by EPR in *a* direction.

Table 5. Eigenvalues of the *g* Tensor in the Crystallographic Direction (g_a, g_b, g_c) and for *s*-**1** and *u*-**1** Molecules ($g_{\|}$, $g_{\perp}$) in *s*-**1**·CH_2Cl_2 and *s*-**1**·CH_2Cl_2, Respectively[a]

	g_a	g_b	g_c	g_{av}	$g_{\|}$	$g_{\perp}$
s-**1**·CH_2Cl_2 (at 4.2 K)	2.362(5)	2.317(5)	2.216(5)	2.298(5)	2.163(5)	2.363(5)
u-**1**·$2CH_2Cl_2$ (at 10 K)	3.69(2)	3.69(2)	2.26(2)	3.21(2)	2.03(2)	3.84(2)

[a] g_{av} is the average value obtained from the principal values.

Table 6. Thermodynamic Parameters and Regression Coefficient (Quality of Fit) Obtained from the Ideal Solution Modeling of the Effective Magnetic Moment for *s*-**1**·CH_2Cl_2

	ΔH (kJ mol^{-1})	ΔS (J K^{-1} mol^{-1})	T_{sc} (K) (= $\Delta H/\Delta S$)	R^2 (regressn coeff)
$S = {}^1/_2 \leftrightarrow S = {}^3/_2$	18.0	54.7	468	0.99803
$S = {}^1/_2 \leftrightarrow S = {}^5/_2$	13.7	29.2	329	0.99988

At this point it is instructive to compare the temperature dependence of μ_{eff} for the different orientations of the crystal of *u*-**1**·$2CH_2Cl_2$. In both directions, small antiferromagnetic interactions between the tricobalt units are evident by a decrease of μ_{eff} below 8 K. In the *c* direction, μ_{eff} is 1.97 μ_B at 10 K and increases gradually to 3.41 μ_B at 300 K without saturation. The μ_{eff} value in the low-temperature regime is in good agreement with an $S = {}^1/_2$ ground state. In the Δ direction, μ_{eff} also increases gradually from 3.20 μ_B at 10 K and saturates to 4.86 μ_B at ~250 K. The $S = {}^1/_2$ ground state was verified by the field dependence of the magnetization in both the *c* and the Δ directions which led to *g* values of 2.26(2) and 3.69(2), respectively. Above 250 K, the saturation of μ_{eff} indicates that the high-spin state of the Co_3 molecule in *u*-**1**·$2CH_2Cl_2$ is $S = {}^3/_2$ with a *g* value of 2.51(2). The *g* factor is very anisotropic and also strongly temperature-dependent, which is not surprising given the documented thermal variation of the structure (Figure 9). The simultaneous occurrence of variations in the *g* factor and a spin-state change precludes a fitting of the magnetic data such as the one presented for *s*-**1**·$2CH_2Cl_2$.

From the single-crystal experiments and the crystal structure at 20 K, the *g* tensors for *u*-**1** molecule are $g_{\|} = 2.03(2)$ and $g_{\perp} = 3.84(2)$ (Table 5). As expected by the differences in metrical parameters of the two molecules, these values are very different from those calculated for *s*-**1**. The *u*-**1** molecule is composed of two Co^{II} atoms joined by a single bond and an "isolated" five-coordinate Co^{II} (Figure 8). This scenario is interpreted as leading to a diamagnetic pair of Co^{II} atoms and an isolated paramagnetic Co^{II}. It follows, then, that the observed spin

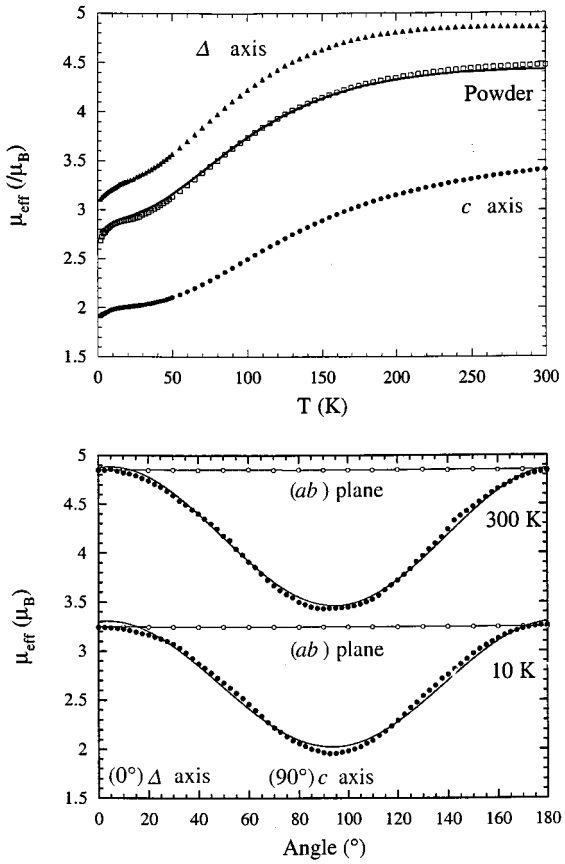

Figure 13. (a) Temperature dependence of the magnetic effective moment for a powder sample and on a single crystal (in the two principal directions) of *u*-**1**·CH_2Cl_2. The continuous line is the temperature dependence of the average effective moment calculated from the single-crystal measurements. (b) Rotation angle patterns of the effective moment at 300 and 10 K in the principal plane *ab* and *c* for *u*-**1**·CH_2Cl_2.

crossover behavior ($S = {}^1/_2$ to $S = {}^3/_2$) is due to the isolated Co^{II} center. This conclusion is in accord with the typical *g* values reported for five-coordinate[25] and distorted octahedral complexes of Co^{II}.[31]

One important aspect in comparing the two compounds is their magnetic behavior and what it reveals about the electronic structure of both molecules. As previously reported,[6] DFT calculations performed on *s*-**1** and *u*-**1** prompted the authors to assign the ground state and first two excited states to be $S = {}^1/_2$ states (doublets). In this study, the calculations revealed that a thermal population of quartet or higher spin states is highly unlikely. Nevertheless in 1994, Peng and co-workers reported[1] the magnetic behavior of the *u*-**1**·$2CH_2Cl_2$·H_2O to be representative of a spin crossover between an $S = {}^1/_2$ ground state and an $S = {}^3/_2$ excited state which begins around 200 K and is incomplete at 300 K. It is important to point out that the magnetic behavior presented by Peng and co-workers[1] does not match the data obtained for the tetragonal form; in fact, their data are very similar to that observed for *s*-**1**·CH_2Cl_2. This lack of correspondence in the independent data from the two groups is likely related to the fact that Peng's sample was probably a mixture of the two isomers. Unfortunately, crystals of the minor product, *u*-**1**·$2CH_2Cl_2$, were subjected to X-ray characterization, and the resulting structure was erroneously used to explain the magnetic data of the impure, bulk material (which contains mostly *s*-**1**·CH_2Cl_2). The single-crystal studies reported in this

(31) Carlin, R. L., Ed. *Magneto-chemistry*; Springer-Verlag: New York, 1986.

work put to rest these purity issues and underscore the importance of firmly establishing that a bulk sample used to measure properties contains only one crystal type.

Concluding Remarks

Low-temperature crystallographic studies have now revealed a second-order phase change for *s*-**1**·CH_2Cl_2, although the Co_3 chain of *s*-**1** remains symmetrical at all temperatures. More significant changes of Co−Co and Co−N distances have been found for *u*-**1**·$2CH_2Cl_2$. At lower temperatures, the short and long metal-to-metal distances become less unsymmetrical, possibly as the result of a high-spin to low-spin transition of the five coordinate Co atom at the terminal position. The magnetic behavior of both *s*-**1**·CH_2Cl_2 and *u*-**1**·$2CH_2Cl_2$ reveal spin crossover behavior from a common ground state $S = {}^1/_2$ to a higher spin state which is clearly $S = {}^3/_2$ for *u*-**1**·$2CH_2Cl_2$ and most likely $S = {}^5/_2$ for *s*-**1**·CH_2Cl_2.

Acknowledgment. The authors acknowledge financial support from the National Science Foundation and the Robert A. Welch Foundation. Work at Argonne National Laboratory was supported by the U.S. Department of Energy, Office of Basic Energy Sciences, Division of Materials Sciences, under Contract W-31-109-ENG-38. The authors thank Professor Claude Coulon for insightful discussions and for the use of the EPR instrument in the Centre de Recherche Paul Pascal (Pessac, France). We are also grateful to Dr. Renald N. Guillemette for recording the SEM images and to Professors Eugenio Coronado and Philipp Gütlich for helpful discussions.

Supporting Information Available: X-ray crystallographic data for *s*-**1**·CH_2Cl_2 and *u*-**1**·$2CH_2Cl_2$ are available in CIF format. Tables of neutron diffraction data for *s*-**1**·CH_2Cl_2 at 20 K, including atomic coordinates, anisotropic thermal parameters, and interatomic distances and angles are also provided (PDF). This material is available free of charge via the Internet at http://pubs.acs.org.

JA000515Q